APLICAÇÃO DA FÓRMULA DE RUDOE NA DETERMINAÇÃO DE LONGAS TRAJETÓRIAS DE ONDAS SÍSMICAS SUPERFICIAIS

Application of Rudoe's Formula in Long Seismic Surface Wave Paths Determination

Newton P. Santos
Jorge L. de Souza

MCT - Observatório Nacional
Gal. José Cristino, 77 – São Cristóvão
20921-400, Rio de Janeiro, Brazil
newton@on.br
jorge@on.br

RESUMO

Um algoritmo é proposto para o cálculo acurado das distâncias pela fórmula de Rudoe, em compartimentos de grade geodésica percorrida por trajetórias de ondas sísmicas superficiais. As coordenadas das interseções das trajetórias com a grade são também obtidas, cujos dados são exibidos em projeção azimutal eqüidistante para simples verificação dos resultados. O modelo adotado para a Terra é o elipsóide de referência GRS-80. O algoritmo fornece as interseções médias, obtidas a partir das seções normais ao elipsóide, diretas e recíprocas, pelo método de Rudoe, cujo afastamento pode ser superior à própria magnitude das células da grade, dependendo do comprimento da trajetória. O método foi testado em um conjunto de dados contendo 3.269 trajetórias fonte-estação, cujos eventos sísmicos foram registrados em 23 estações da rede IRIS. As distâncias entre estação e epicentro variam entre 1.634 km e 16.400 km, cujos limites da área são, respectivamente, 149°E × 21°W e 50N × 90°S. Os resultados mostram que a acurácia das interseções estimadas depende do azimute da trajetória e da latitude, cuja influência pode ser significativa para distâncias muito longas, como é o caso em aplicações telesísmicas, o que indica o emprego do algoritmo proposto.

Palavras chaves: Geodésia; Sismologia; Tomografia com velocidade de grupo; Trajetórias telesísmicas; Sistema GRS-80.

ABSTRACT

An algorithm to compute accurate distances over grid cells crossed by seismic surface wave paths by Rudoe's formula is proposed. The intersection coordinates between paths and the geodetic grid are also computed, which data are exhibited in an azimuthal equidistant projection to check the results. GRS-80 is the adopted ellipsoidal Earth model. The algorithm computes the intermediate intersections, from both forward and reciprocal normal sections given by Rudoe's method, which separation may be greater than the cell size. It was tested on a data set including 3,269 source-station paths, which seismic events were recorded at 23 IRIS stations. The epicentral distances range from 1,634 km to 16,400 km, which the grid spreads over 149°E × 21°W, and 50N × 90°S. The results show that the estimated intersections accuracy depends on the path azimuth and latitude, which influence may be significative for very long distances as in teleseismic applications, which argues for the algorithm application.

Keywords: Geodesy; Seismology; Group velocity tomography; Teleseismic paths; GRS-80.

1. INTRODUCTION

Recent technological advances in seismometry, data recording, transmission and access have led to the development of a new generation of global networks prepared to detect the seismic phenomena over a broad range of frequencies. These include networks installed by the Incorporated Research Institutions for Seismology (IRIS) Consortium, GEOSCOPE and GEOFON.

Seismic station distribution in the South America continent and adjacent areas, in particular, is far from an ideal one for a local experiment with seismic body wave tomography (P and/or S waves), but it allows for the development of regional seismic surface wave tomography investigations.

It is well known in seismic surface wave tomography that source-station paths' density is an important parameter to get consistent results. However, in local studies, we are dealing with long source-station paths and we are investigating small portions of the total paths. Thus, it is necessary to have a hard control on both partial and total distances in a gridded area.

In general, seismologists use a spherical model to compute the distance between two particular points on the Earth surface and, afterwards, they apply some approximate expressions to correct the ellipsoid flattening (KENNETH, 2002; THOMAS, 1965). Furthermore, this procedure is normally used only to compute the source-station distances, but might be a drawback to calculate the grid intersections accurately. In the presented study, an algorithm computes all distances with high accuracy for seismological applications, which are obtained directly in the ellipsoidal Earth model. This procedure is completely different from that commonly applied in Seismology. Thus, the proposed algorithm may be viewed as an alternative approach to insure a high precision of the estimated group velocities. It applies the Rudoe's formula in order to get high accuracy, either in the source-station distance or in the geodetic grid intersections.

This investigation also follows a recommendation of the International Union of Geodesy and Geophysics - IUGG (MORITZ, 1980), in order to adopt the GRS-80 ellipsoid for all purposes in geodetic and geophysical applications.

2. THE SEISMOLOGICAL PROBLEM

Let's consider a seismic surface wave path between a seismic source and a station, without significant lateral variation. Thus, it is projected as a straight line onto a plane. We are interested in computing both total and partial lengths (distance into grid cells) with high accuracy for using in surface wave tomographic problems.

Supposing many seismic stations and events (i.e., P source-station paths) distributed in a gridded area (C cells), let's assume that, for a given path, the total time delay is equal to the sum of partial time delays across the cells. Thus, for a particular period T (or frequency) and path j, we have (FENG AND TENG, 1983)

$$\frac{1}{U^j} - \frac{1}{V^j} = \sum_{i=1}^{nC} \frac{d_i^j}{D^j}\left[\frac{1}{u^i} - \frac{1}{v^i}\right] \qquad j = 1,\ldots,nP \qquad (1)$$

where U^j and V^j are, respectively, the observed and theoretical source-station group velocities, D^j is the source-station distance, and d_i^j, u^i, v^i are, respectively, distance and group velocities at cell i (estimated and theoretical). Eq. (1) represents a typical seismic surface wave group velocity tomographic problem in Seismology. The accurate computation of total (D^j) and partial distances (d_i^j) is the aim of this study.

2.1 Representation of the results

An azimuthal and equidistant projection is used here in order to visualize and check the results, because data are computed in true scale. This projection preserves both distances and directions taken from the origin (BOMFORD, 1971; PEARSON, 1990; RICHARDUS AND ADLER, 1972; SNYDER, 1982). Herein, the projection surface is a plane tangent to the model at origin, and the lengths taken from the origin are represented as straight lines with no distortion.

The Geodetic Reference System - 1980 ellipsoid (GRS-80) is used as the Earth model (MORITZ, 1984), in order to get minimum cartographical errors. Indeed, despite a spherical model may be considered sufficient for regional body wave tomographic applications (JULIAN *et al.*, 2000), the differences between both models might reach up to a few quilometers for very long distances, as for teleseismic applications.

The seismic surface wave lengths are computed by Rudoe's formula (BOMFORD, 1971). Nevertheless, as Rudoe's formula yields distance along an ellipsoid normal section – and not along the geodetic line – there were differences on the points in which grid cells are intersected by a path. This is troublesome when comparing forward and reciprocal station-to-epicenter directions, because those differences may be significative, depending on the cell size. If the cell size is on the same magnitude as those differences, it may mask the result itself. In the presented algorithm, an intermediate path is computed from both forward and reciprocal intersections in order to produce the minimal differences.

Because of the ellipsoid geometry, the normal section at a point P_1 that contains another point P_2, is not the same as its reciprocal (P_2 to P_1). Both normal sections cut the ellipsoid surface at different planes, leading to distinct curves. The geodetic is a double curved line between them. However, as both the geodetic line and the normal section length differ very slightly [This difference is about 1/150 ppm at 3,000 km (BOMFORD, 1971)], we might use the normal section length as the distance between two points, instead of the geodetic line, and the intermediate path for the intersections with the grid.

2.2 Rudoe's Formula

Rudoe's formula is the most accurate method to compute distances and azimuths, suitable for any

distance, and it is used as a standard of comparison with the others. It is based on the reckoning of normal section lengths between two points on the ellipsoid surface. We will transcribe it here, extended to give rectangular coordinates x and y (x-axis increases easterly, and y-axis increases northerly).

Firstly, azimuth Az to forward direction (east of north at origin) is calculated from Cunningham's closed formula (BOMFORD, 1971),

$$\cot Az = (\Lambda - \cos\Delta\lambda)\sin\phi_s \operatorname{cosec}\Delta\lambda \tag{2}$$

where

$$\Lambda = \frac{\tan\phi_E}{(1+\varepsilon)\tan\phi_S} + e^2 \frac{N_S \cos\phi_S}{N_E \cos\phi_E} \tag{3}$$

In Eq. (3), e and ε are, respectively, the first and second eccentricity of the ellipsoid, and N is the radius of curvature in the plane perpendicular to the meridional plane at the point (the radius of the first vertical section). These quantities are defined as

$$e^2 = \frac{a^2 - b^2}{a^2} \tag{4}$$

$$\varepsilon^2 = \frac{e^2}{1-e^2} \tag{5}$$

$$N = \frac{a}{\sqrt{1 - e^2 \sin^2\phi}} \tag{6}$$

where a is the semimajor axis of meridian ellipse (equatorial radius), and b is the semiminor axis (polar radius).
Indices S and E refer to the station and epicenter, respectively, and ϕ and λ are their geodetic coordinates. Also, in Eq. (2), we have $\Delta\lambda = \lambda_E - \lambda_S$.

The principle in Rudoe's technique is the computation of semiminor axis and second eccentricity of the ellipse in which the normal section cuts the ellipsoid at origin.

$$b_0 = \frac{N_S}{1+\varepsilon}\sqrt{1 + \varepsilon \cos^2\phi_S \cos^2 Az} \tag{7}$$

$$\varepsilon_0 = \varepsilon\left(\cos^2\phi_S \cos^2 Az + \sin^2\phi_S\right) \tag{8}$$

Therefore, we get reduced latitudes u'_S and u'_E in this ellipse, at the station and epicenter, respectively,

$$\tan u'_S = \frac{\tan\phi_S}{\cos Az\sqrt{1+\varepsilon_0}} \tag{9}$$

$$\tan u'_E = \frac{\mathrm{N_S}\sin\phi_\mathrm{S} + (1+\varepsilon_0)(z_E - z_S)}{(x_E \cos Az - y_E \sin\phi_\mathrm{S} \sin Az)\sqrt{1+\varepsilon_0}} \tag{10}$$

where

$$x_E = N_E \cos\phi_E \cos\Delta\lambda \tag{11}$$

$$x_E = N_E \cos\phi_E \sin\Delta\lambda \tag{12}$$

$$z_E = N_E(1-e^2)\sin\phi_\mathrm{E} \tag{13}$$

$$z_S = N_S(1-e^2)\sin\phi_\mathrm{S} \tag{14}$$

Normal section length, i.e., the geodetic distance apart the origin (station) is

$$L = b_0\left[c_0(u'_E - u'_S) + c_2(\sin 2u'_E - \sin 2u'_S) + c_4(\sin 4u'_E - \sin 4u'_S)\right] \tag{15}$$

where

$$c_0 = 1 + \frac{1}{4}\varepsilon_0 - \frac{3}{64}\varepsilon_0^2 + \frac{5}{256}\varepsilon_0^3 \tag{16}$$

$$c_2 = -\frac{1}{8}\varepsilon_0 + \frac{13}{32}\varepsilon_0^2 - \frac{15}{1024}\varepsilon_0^3 \tag{17}$$

$$c_4 = -\frac{1}{256}\varepsilon_0^2 + \frac{3}{1024}\varepsilon_0^3 \tag{18}$$

The rectangular coordinates of a given point are

$$\begin{cases} x = L\ sin\ Az + x_0 \\ y = L\cos Az + y_0 \end{cases} \tag{19}$$

where x_0 and y_0 are the origin plane coordinates.

2.3 The Algorithm

As we have seen, we may use either the normal sections as good approximations of the distance, instead of the geodetic line. Nevertheless, as those curves take different paths in both forward and reciprocal directions (or azimuths), the cells are crossed into two different paths, and the intersections are not the same in both directions. To resolve this, we can get the intermediate path between them (as the geodetic line) to estimate the grid intersections with very good approximation.

Plotting the grid intersections in the azimuthal and equidistant projection to the forward, reciprocal and intermediate paths, respectively, in a graph (taking station or epicenter as the origin), we get a straight line joining the intersections for the forward path, and curved lines for the others. The intermediate path is the solution we are finding out. The plane coordinates of the intersections are the same whatever the origin, which is used as a computational check. Evidently, each path is computed twice, one to the forward direction and the other to its reciprocal, and the algorithm deals with as many systems as the double of the number of paths. The intermediate path is not a straight line, but so each segment that crosses a cell.

2.4 An Example

The following illustration (Fig. 1) is an example to visualize a particular source-station path in an azimuthal and equidistant projection. It crosses the grid which is limited by meridians 35°E and 115°W, and parallels 30°N and 35°S, and was further subdivided into cells of 5°×5°. It refers to IRIS Southerland station (South Africa) as origin, which coordinates are 32.4°S and 20.8°E, and the epicenter at 26.2°N and 110.5°W. The algorithm was implemented in Fortran code, whose distances are 15,286.820 km and 15,286.856 km, respectively, to forward and reciprocal paths. The difference is 0.036 km (0.0002% or 2 ppm), which is negligible in this example.

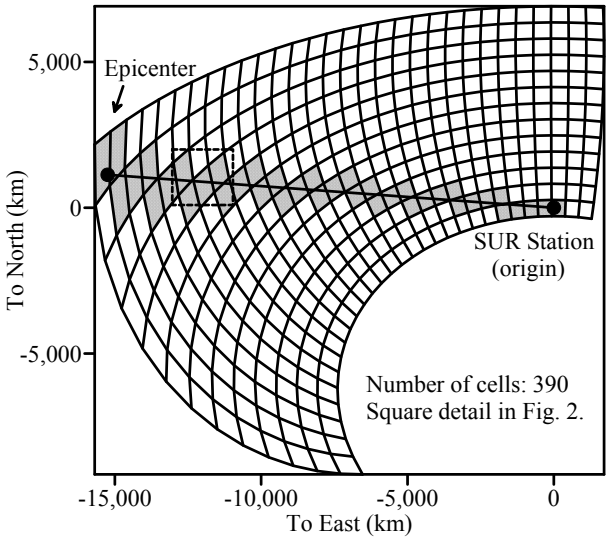

Fig. 1 - Wave path of length 15,287 km represented in an azimuthal and equidistant projection.

The routine gives the distances within each cell crossed by this wave path, as well as the normal sections separation between forward and reciprocal paths. In this projection, the grid is strongly distorted, mainly for points far from the origin. The exception is the origin-meridian, projected as a straight line in a true scale.

The whole data set, including 3,269 source-station paths, were also tested, giving RMS difference, mean difference and standard deviation, respectively, equal to 0.007 km, -0.002 km and 0.007 km. The minimum and maximum absolute differences are 0 km and 0.081 km, respectively. The minima differences occur for 2,434 source-station paths, and the maximum difference occur for one path, which length is equal to 12,809 km.

Eventually, depending on either station or epicenter position, some cells crossed in a given direction may not be crossed in its reciprocal (sometimes, neither in the intermediate one). This is due to the ellipsoid geometry. That is the case of cell #96, in Fig. 2, which displays an enlarged detail of the grid (see Fig. 1).

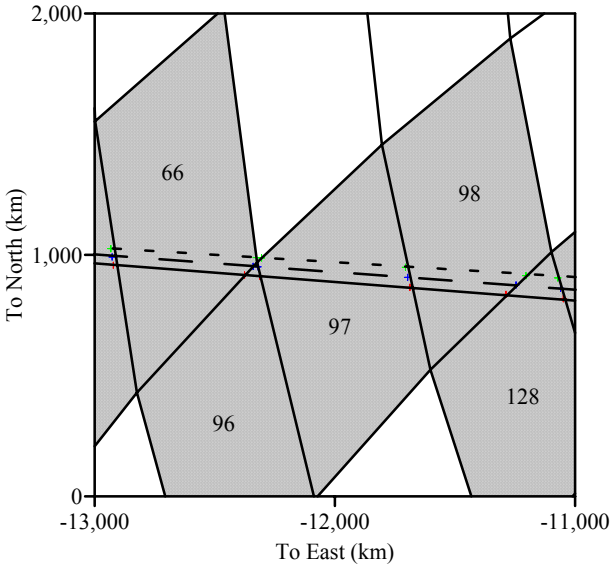

Fig. 2 – Detail of the grid. Lines crossing the cells represent, respectively, forward (continuous), intermediate (dashed) and reciprocal (dotted) paths.

The linear separation between forward and reciprocal normal sections for the path figured in this example, is presented in a top-view graph (Fig. 3). Vertical axis shows the separations, and horizontal axis shows the distances apart Southerland station, as well as the sucessive grid intersections. In this case, the maximum separation is 86.5 km, which represents 0.57% of deviation. As already said, the intersection coordinates are the same whatever the origin.

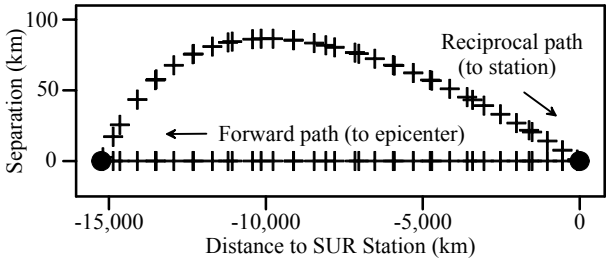

Fig. 3. Separation between forward and reciprocal normal sections for the path in Fig. 1. Pluses represent grid intersections. Vertical axis exagerated.

3. RESULTS

The algorithm was tested on a data set including 3,269 source-station paths, corresponding to 1,132 events recorded at 23 IRIS seismic stations. The area spreads over 21°E × 149°W, and 50° N × 90° S, which lengths range between 1,634 km and 16,400 km. For the experiment, the grid was subdivided into cells of sizes 10°×10°, 5°×5°, 2°×2° and 1°×1°, respectively, which are the most usable grid spacing in Seismology.

The separation lengths between forward and reciprocal normal sections were computed (Fig. 4), as well as their correlation with path length (a) and path azimuth (b). As both forward and reciprocal intersections are not the same in the most cases, due to

the relative station and epicenter positions and distances, the intermediate intersections were computed.

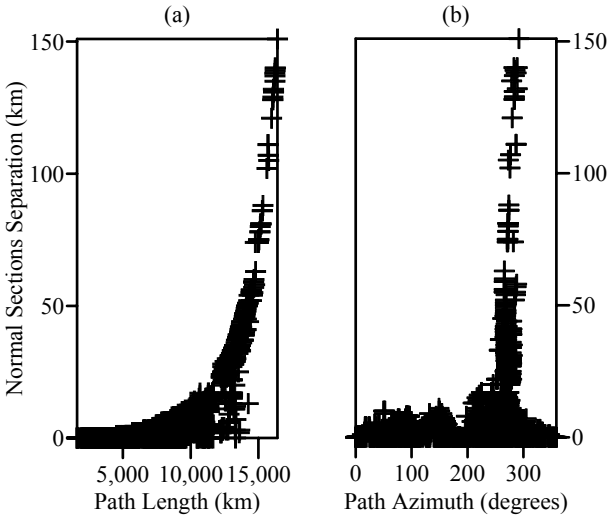

Fig. 4 - Correlation between normal sections separation with path lengths (a), and path azimuths (b). Vertical axis exagerated in (a).

Fig. 4 shows that, in general, normal sections separation increases with path length, although it depends strongly on the azimuth. For example, small values (0-20 km) for very long distances (12,000-13,000 km) refer to the paths which are near the Equator, wherein the normal sections are close to each other. In other cases, the separation reachs up to 150 km. Fig. 4 (b) shows that the largest separations correspond to azimuths near 270°. In this case, separation increases with distance for the same azimuth. The smallest values correspond to azimuths near 0° or 180° (whatever the path length), and for azimuths close to 90° or 270°, when the path is near the Equator. In all other cases, separation increases with path length, whatever the station or epicenter location. As an example, the largest separation (151 km) corresponds to the longest path length (16,416 km) for the station at latitude 32.4°S, in South Africa (see Fig. (1). The peaks around $Az = 270°$ (Fig. 4 (b)) refer to the paths to this station. In short, the results show that for path lengths longer than approximately 12,000 km, the dependence with path azimuth is significative, while for path lengths smaller than this value, the azimuthal dependence is weaker. Also, for this data set, normal sections separation is equal to 16 km at most for path lengths smaller than approximately 8,900 km.

As an illustration, both graphs in Fig. 4 are merged into the 'bubble' plot (Fig. 5), as a 3D chart. It shows the simultaneous correlation of normal sections separation with both path length and path azimuth.

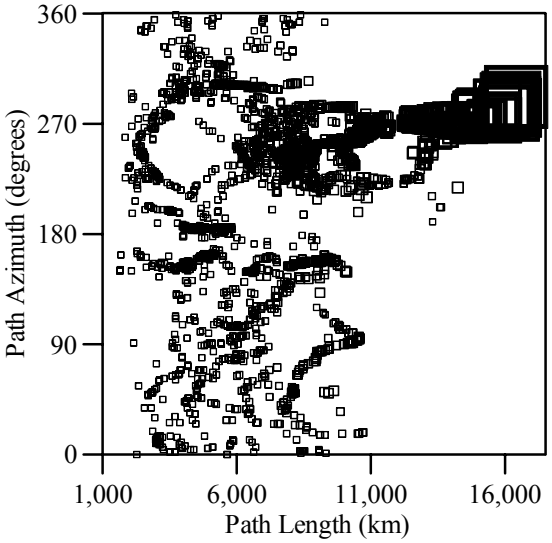

Fig. 5. Variation of normal sections separation with path length and path azimuth, simultaneously. Square's size indicates separation magnitude (km).

Using a subset of these data, the algorithm was also applied in three-dimensional S-wave velocity structure studies (group velocity tomography) in Southeastern Brazil (PACHECO, 2003; SOUZA *et al*., 2003; SOUZA AND SANTOS, 2003), Northeastern Brazil (VILAR *et al.*, 2003; VILAR, 2004), and in the São Paulo Plateau area (BORBA JÚNIOR, 2001). In these studies, as in other papers (see, e.g., FENG AND TENG, 1983), the surface waves are assumed as propagating exactly along the geodetic line in true scale, thus the chosen grid cell sizes only serve to subdivide the source-station path into segments. It is worth to mention that the cell size is merely a seismological problem. That is, the grid spacing depends on the type of seismic surface wave data available, i.e., local, regional or global data. New methods (such as Fresnel-area ray tracing - FRT) have been proposed in the literature to take into account the lateral variation of a seismic surface wave path between a source and a station (see, e.g., YOSHIZAWA AND KENNETT, 2002).

In order to analyze the routine performance, processing time was tabulated (Table 1) for each path length crossing the grid cells, in sizes 10°×10°, 5°×5°, 2°×2° and 1°×1°, respectively. The test runs on a PC Pentium III 800/128 MB. Column "#Cells" indicates the number of grid cells, and "RMS" and "Total" represent, respectively, the Root Mean Square and total processing times to compute all the paths. Both columns "Minimum" and "Maximum" refer to the shortest and to the longest path lengths, respectively.

TABLE 1 – ROUTINE PROCESSING TIME (SECONDS) ON A PC PENTIUM III 800/128 MB.

Cell Size	10°×10°	5°×5°	2°×2°	1°×1°
#Cells	238	952	5,950	23,800
Minimum	.00	.00	.00	.05
Maximum	.11	.17	.66	2.15
RMS	.03	.04	.12	.40
Total	1.38	3.31	12.58	39.80

4. CONCLUSIONS

Because it is based on the well-known Rudoe's formula, the presented algorithm has to be as accurate as possible, as well as efficient to compute the source-station distances. It also computes the intersections between teleseismic wave paths and the geodetic grid. Considering the results obtained, either in the tests or in the real situations, we might conclude that the proposed algorithm, based on the ellipsoidal Earth model, may be used as an alternative approach in teleseismic problems, instead of the usual ellipticity correction applied to a spherical model. Rudoe's method showed to be an adequate choice for the computation, taking into account the magnitude of the studied path lengths, which range between 1,634 km and 16,400 km. The results also emphasized that for path lengths longer than approximately 12,000 km, the azimuthal dependence is rather pronounced, which justify the algorithm application further, in order to insure the grid intersections accuracy. The algorithm also might be used for any grid subdivision, as well as for irregularly grid spacing. This is because the grid cell size is merely a seismological, but not a cartographical subject, which depends basically on the type of seismic surface wave data available.

ACKNOWLEDGMENTS

The authors would like to thank Incorporated Research Institutions for Seismology (IRIS) for providing all data set used in this study, as well as Fundação de Amparo à Pesquisa do Estado do Rio de Janeiro (FAPERJ) and MCT / Observatório Nacional for all supporting. They also thank to the anonymous reviewers for their helpful comments and valuable suggestions.

REFERENCES

BOMFORD, G.. **Geodesy**. Oxford University Press, 3rd Edition, 1971. 731 p.

BORBA JUNIOR, A. **Estrutura Litosférica do Platô de São Paulo Derivada a Partir de Ondas Sísmicas Superficiais**. M.Sc. dissertation, MCT/ Observatório Nacional, 2001. 185 p.

FENG, C.C.; TENG, T.L. Three-Dimensional Crust and Upper Mantle Structure of the Eurasian Continent. **Journal of Geophysical Research,** v. 88 (B3), p. 2261-2272, 1983.

JULIAN, B. R.; EVANS, J. R.; PRITCHARD, M. J.; FOULGER, G. R.. A Geometrical Error in Some Computer Programs Based on the Aki-Christoffersson-Husebye (ACH) Method of Teleseismic Tomography. **Bulletin of Seismological Society of America**, v. 90, n. 6, p. 1554-1558, 2000.

KENNETH, B. L. N. **The Seismic Wavefield. Vol. II: Interpretation of Seismograms on Regional and Global Scales**. Cambridge University Press, 2002. 534 p.

MORITZ, H.. Geodetic Reference System 1980. **Bulletin Géodésique**, v. 58, n. 3, p. 388-398, 1984.

PACHECO, R. P. **Imageamento Tridimensional da Onda S na Litosfera do Sudeste Brasileiro e Adjacências**. Rio de Janeiro, Tese de Doutoramento, MCT/ Observatório Nacional, 2003. 495 p.

PEARSON, F. II. **Map Projections: Theory and Applications**. Boca Raton, Florida, CRC Press, Inc., 1990. 372 p.

RICHARDUS, P.; ADLER, R. K. **Map Projections for Geodesists, Cartographers and Geographers**. Amsterdam, North-Holland Publishing Co., 1972. 174 p.

SNYDER, J. P. **Map Projections Used by the U. S. Geological Survey.** U. S. Geological Survey Bulletin, 1532, 1982. 313 p.

SOUZA, J. L. de; SANTOS, N. P.; PACHECO, R. P. Regionalized Rayleigh Wave Group Velocities in Southeastern Brazil. **Geophysical Research Abstracts**, v. 5, p. 1681, 2003.

SOUZA, J. L. de.; SANTOS, N. P. Tomografia com Velocidade de Grupo de Ondas Rayleigh na Região Sudeste do Brasil. 8th International Congress of the Brazilian Geophysical Society and 5th Latin American Geophysical Conference, Rio de Janeiro, 2003. **CD-ROM**.

THOMAS, P. D. Geodesic Arc Length on the Reference Ellipsoid to Second-Order Terms in the Flattening. **Journal of Geophysical Research**, v. 70, n. 14, p. 3331-3340, 1965.

VILAR, C. S. **Estrutura Tridimensional da Onda S na Litosfera do Nordeste Brasileiro**. Rio de Janeiro, Tese de Doutoramento, MCT/ Observatório Nacional, 2004. 258 p.

VILAR, C. S.; SOUZA, J. L. DE; SANTOS, N. P. Tomografia com Velocidade de Grupo de Ondas Rayleigh na Região Nordeste do Brasil. 8th International Congress of the Brazilian Geophysical Society and 5th

Latin American Geophysical Conference, Rio de Janeiro, 2003. **CD-ROM**.

YOSHIZAWA, K.; KENNETT, B. L. N. Determination of the influence zone for surface wave paths, **Geophysical Journal International**, v. 149, p. 440-453, 2002.

Recebido em 30 de maio de 2005 – Aceito para publicação em 30 de dezembro de 2005.